



## Proton Transfer in a Two-Dimensional Hydrogen-Bonding Network: Water and Hydroxyl on a Pt(111) Surface

M. Nagasaka,<sup>1,2</sup> H. Kondoh,<sup>1,\*</sup> K. Amemiya,<sup>1,3</sup> T. Ohta,<sup>1,4</sup> and Y. Iwasawa<sup>1</sup>

<sup>1</sup>Department of Chemistry, Graduate School of Science, The University of Tokyo, 7-3-1 Hongo, Bunkyo-ku, Tokyo 113-0033, Japan

<sup>2</sup>Institute for Molecular Science, Myodaiji, Okazaki 444-8585, Japan

<sup>3</sup>Institute of Materials Structure Science, Tsukuba, Ibaraki 305-0801, Japan

<sup>4</sup>SR Center, Ritsumeikan University, 1-1-1 Noji-Higashi, Kusatsu, Siga 525-8577, Japan

(Received 17 November 2007; published 10 March 2008)

The time scale of proton transfer between H<sub>2</sub>O and OH adsorbed on a Pt(111) surface was determined by a combination of laser-induced thermal desorption (LITD) and microscale x-ray photoelectron spectroscopy (micro-XPS). The patterned distribution OH + H<sub>2</sub>O/H<sub>2</sub>O/OH + H<sub>2</sub>O was initially prepared on the Pt(111) surface by the LITD method and the time evolution of the spatial distribution of H<sub>2</sub>O and OH was observed by the micro-XPS technique. From quantitative analyses based on a diffusion equation, we found two proton-transfer pathways with different time scales of  $5.2 \pm 0.9$  ns and  $48 \pm 12$  ns at 140 K, which were attributed to direct proton transfer to the neighbor site and H<sub>3</sub>O<sup>+</sup>-mediated transfer to the next-nearest site, respectively.

DOI: 10.1103/PhysRevLett.100.106101

PACS numbers: 68.43.Jk, 68.37.Xy, 82.65.+r

Proton transfer in hydrogen bonded systems is one of fundamental processes in nature and plays significant roles in many physical, chemical, and biological processes, such as solvation [1], proton conductive polymer electrolyte [2], acid-base reaction [3], catalyst [4], and enzymatic reaction [5]. It is also a key process for “protonics” that is the alternative of electronics [6]. The time scale of the proton transfer is essential for understanding the above processes and it is challenging to determine the transfer rate experimentally. Recently, Katoh *et al.* measured the proton transfer in highly pressurized ice by infrared reflection (IR) spectroscopy [7]. Water molecules form well-ordered two-dimensional (2D) networks on metal surfaces [8]. Because the 2D ice supported by a metal surface is energetically stable, it is a promising system to study the proton transfer in the 2D hydrogen-bonding network.

Water formation from oxygen and hydrogen on a platinum surface is one of the well-known catalytic reactions and has attracted much attention recently because it is the key reaction for a practical fuel cell [8]. The reaction mechanism has been extensively investigated by using model systems; for example, an oxygen-precovered Pt(111) surface was exposed to hydrogen gas to form water molecules [9]. During the reaction, the OH species appears as an intermediate [10]. Recent temperature programmed desorption measurements revealed that the OH species does not exist as a pure OH phase but forms a mixed overlayer with H<sub>2</sub>O [11]. Figure 1(a) shows a structure of the mixed overlayer, where both OH and H<sub>2</sub>O occupy the atop sites of Pt(111) [12], with a honeycomblike structure [13]. Density functional theory calculations suggested a facile proton transfer from H<sub>2</sub>O to OH in the mixed OH + H<sub>2</sub>O overlayer [14]. The presence of the proton transfer in the mixed overlayer was also evidenced by broadening of the O-H bending mode with the IR spectroscopy [11]. Recently, we applied the kinetic Monte Carlo simulation

method to the water formation reaction on Pt(111), and found a possibility that the proton transfer has a significant role to supply H<sub>2</sub>O (autocatalytic reactant) to the reaction front [15]. However, any firm evidence has not been obtained for actual long-range mass transport by the 2D proton transfer. Furthermore, the time scale of the proton transfer in such a 2D hydrogen-bonding network is still unknown.

In this study, the rate of the proton transfer between H<sub>2</sub>O and OH on a Pt(111) surface was investigated by the combination of laser-induced thermal desorption (LITD) and microscale x-ray photoelectron spectroscopy (micro-XPS). A one-dimensional (1D) pattern consisting of H<sub>2</sub>O and OH, OH + H<sub>2</sub>O/H<sub>2</sub>O/OH + H<sub>2</sub>O, was prepared on Pt(111) by the LITD method as illustrated in Fig. 1(b). The OH coverage in the central H<sub>2</sub>O region is expected to increase by the proton transfer, which can be examined by the time evolution of OH and H<sub>2</sub>O distributions monitored with micro-XPS. From quantitative analyses of the distribution change, we estimated the time scale of the

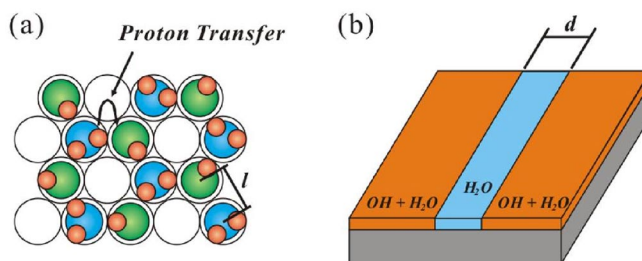


FIG. 1 (color online). (a) Schematic model of proton transfer between H<sub>2</sub>O and OH in the mixed OH + H<sub>2</sub>O overlayer on Pt(111). The distance  $l$  of unit cell is 2.8 Å. (b) Schematic of 1D surface modulated distribution OH + H<sub>2</sub>O/H<sub>2</sub>O/OH + H<sub>2</sub>O on Pt(111). The width of H<sub>2</sub>O region  $d$  was 400 μm.

proton transfer in the mixed OH + H<sub>2</sub>O overlayer on Pt(111), and found two different paths of proton transfer.

The experiments were performed at soft x-ray beam line, BL-7A [16] of the Photon Factory, High Energy Accelerator Research Organization (KEK-PF), using an ultrahigh vacuum system (below  $1.0 \times 10^{-10}$  Torr). First, an oxygen-covered Pt(111) surface was prepared by exposing to 30 L (1 L =  $1.0 \times 10^{-6}$  Torr s) O<sub>2</sub> gas at 120 K, followed by annealing at 240 K. This surface was exposed to 5 L H<sub>2</sub>O at 130 K, and annealed at 175 K. As a result, the mixed OH + H<sub>2</sub>O phase was formed on a Pt(111) surface [Fig. 1(a)]. Under this condition, the ratio of OH and H<sub>2</sub>O becomes 2:1, and the total coverage of the mixed phase is 0.75 ML [11] as was confirmed by XPS.

To prepare the 1D spatial distribution of adsorbates, OH + H<sub>2</sub>O/H<sub>2</sub>O/OH + H<sub>2</sub>O, as shown in Fig. 1(b), the pristine OH + H<sub>2</sub>O mixed overlayer was patterned by LITD using a pulsed laser beam [*Q*-switched Nd: yttrium aluminum garnet (wavelength: 532 nm, duration time: 5 ns)]. The laser beam was focused into a small spot 400  $\mu\text{m}$  in diameter by a lens with a focal length of 300 mm located outside the chamber. The sample was scanned along one direction to make a 1D vacant band. To avoid the laser-induced surface damage, the laser power was reduced to 7 mJ/pulse, which was as low as possible to remove the mixed OH + H<sub>2</sub>O overlayer. Then, the patterned surface was exposed to 2 L H<sub>2</sub>O at 130 K for filling the vacant area with H<sub>2</sub>O, and subsequently annealed at 160 K to remove excess H<sub>2</sub>O. In the pure H<sub>2</sub>O overlayer, H<sub>2</sub>O molecules also occupy atop site, and form the same honeycomb structure [17]. The distributions of OH and H<sub>2</sub>O were measured by O 1s XPS spectra with an excitation energy of 630 eV. The kinetic energy of the emitted electron was measured by using a position sensitive electron energy analyzer. The coverage changes of OH and H<sub>2</sub>O were monitored with a spatial resolution of 16.5  $\mu\text{m}$  at 140 K.

The top of Fig. 2 shows the micro-XPS image obtained from the initial distribution of the 1D pattern of adsorbates OH + H<sub>2</sub>O/H<sub>2</sub>O/OH + H<sub>2</sub>O [18]. The width of the central H<sub>2</sub>O region was 400  $\mu\text{m}$ . To obtain the coverage distribution of OH and H<sub>2</sub>O on the surface, these XPS spectra were fitted by the standard spectra of OH and H<sub>2</sub>O. The peak position of OH and H<sub>2</sub>O are 530.2 and 531.8 eV, respectively. Each XPS spectrum taken from the image is shown in the bottom of Fig. 2. The mixed OH + H<sub>2</sub>O region (A) consists of OH and H<sub>2</sub>O, whose ratio is 2:1. In the border region (B), the OH coverage is lower, while the H<sub>2</sub>O coverage is higher instead. In the central H<sub>2</sub>O region (C), only H<sub>2</sub>O molecules exist on the surface. After 16.3 h, OH species appears in this region at 140 K as shown in (D).

Figure 3 (top) shows the OH and H<sub>2</sub>O coverage distributions at 140 K with different elapsed times. In the central region, OH coverage increases while H<sub>2</sub>O coverage decreases with time. Note that OH species does not diffuse at

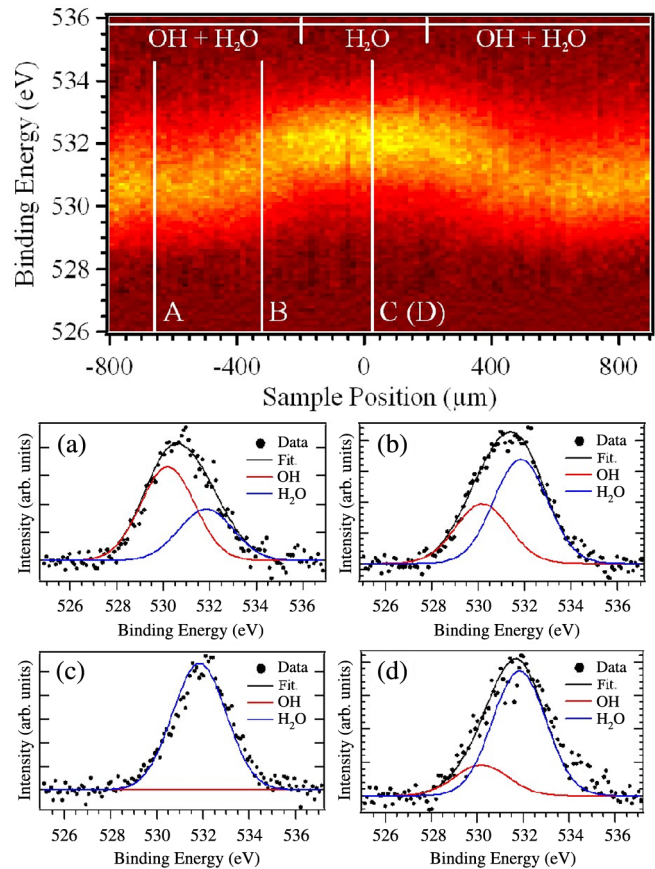


FIG. 2 (color online). (Top) The image of XPS spectra obtained from the initial distribution of the 1D modulated OH + H<sub>2</sub>O/H<sub>2</sub>O/OH + H<sub>2</sub>O structure. The horizontal and vertical axes of the image correspond to the surface position and the binding energy of XPS spectra, respectively. (Bottom) The XPS spectra taken from the different positions of the surface, as indicated in the top figure. The spectra (A),(B), and (C) were taken from the initial distribution. The spectrum (D) was taken after 16.3 h, showing the increase of OH coverage.

140 K, as confirmed by scanning tunneling microscopy experiment [10]. We also confirmed that the appearance of OH is not due to x-ray-induced dissociation of H<sub>2</sub>O by the fact that long-period x-ray irradiation on a pure H<sub>2</sub>O overlayer does not cause formation of OH. Thus, the OH species observed in the central region results from the proton transfer from H<sub>2</sub>O to OH.

From obtained distribution changes, we estimated the rate of proton transfer based on the diffusion equation. First, only a simple proton transfer was considered, where H<sub>2</sub>O and OH exchange their positions when they are located at two adjacent sites as illustrated in Fig. 4(a). If a single OH is mixed in the H<sub>2</sub>O network, the OH species freely travels in the H<sub>2</sub>O network by the proton transfer and vice versa. In the 1:1 mixed OH + H<sub>2</sub>O phase shown in Fig. 1(a), however, this pathway is significantly suppressed, because once a proton hops to the adjacent avail-

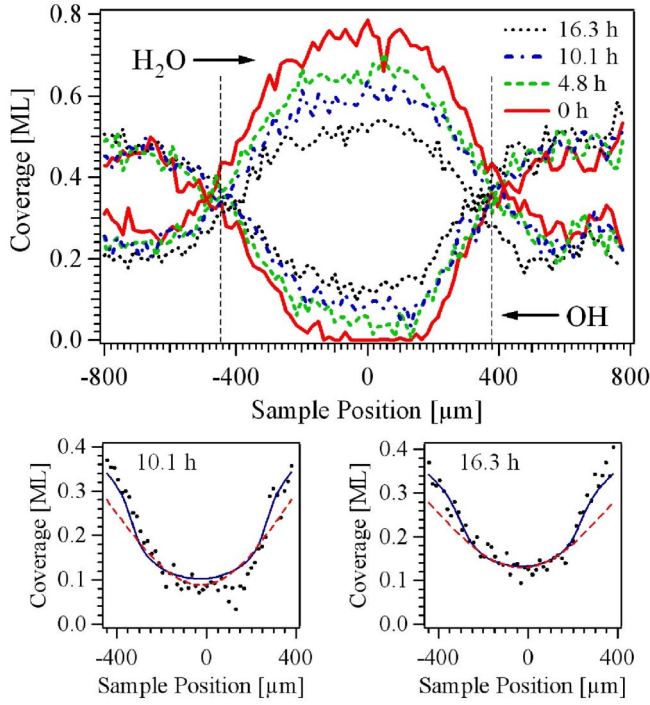


FIG. 3 (color online). (Top) The coverage distribution of OH and H<sub>2</sub>O obtained from surface modulated structure with different elapsed times. The region between two dashed lines was used for fitting. (Bottom) The OH coverages after 10.1 and 16.3 h are shown with the fitted curves: Two processes with the coverage dependence (solid lines), and simple proton transfer without the coverage dependence (dashed lines).

able site, it cannot find a next available site. This confinement prevents the OH/H<sub>2</sub>O species from traveling in the 1:1 mixed phase. Nevertheless, our experiments show the increase of OH coverage in the central region of the modulated structure. Another path of proton transfer should be taken into account, which proceeds even in the 1:1 mixed phase. As a possible process to satisfy this condition, we assume a pathway in which a proton of H<sub>2</sub>O moves to next-nearest OH via H<sub>3</sub>O<sup>+</sup> formation, as shown in Fig. 4(b). This pathway was also proposed by previous molecular dynamics simulation [19]. The probability for this second path has a maximum at the 1:1 mixed phase (0.33 ML), when in contrast the first path has a minimum probability, as shown in the inset of Fig. 4. By assuming two pathways of proton transfer with the proceeding probability, the diffusion equation of OH coverage (OH( $x, t$ ) =  $N$ ) for proton transfer is formulated as [20]

$$\frac{\partial N}{\partial t} = D \left[ \frac{\partial^2 N}{\partial x^2} + (1 - \alpha)(27N^2 - 12N) \frac{\partial^2 N}{\partial x^2} + (1 - \alpha)(54N - 12) \left( \frac{\partial N}{\partial x} \right)^2 \right], \quad (1)$$

where the term  $D$  is the diffusion coefficient of first process, and that of second process is set to be  $\alpha$  times larger

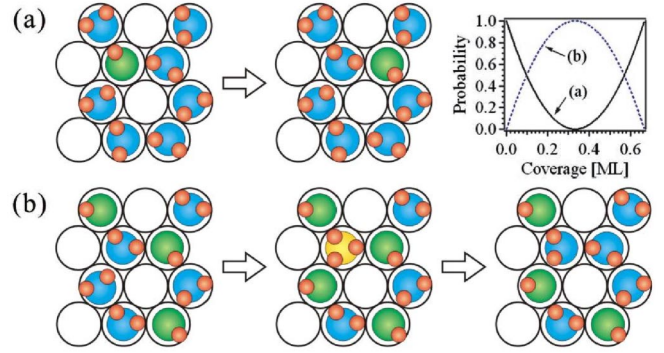


FIG. 4 (color online). The schematics of two process of proton transfer: Simple proton transfer (a), and proton transfer via H<sub>3</sub>O<sup>+</sup> species (b). In the right upper part, the proceeding probabilities of the two processes are shown as a function of the coverage.

than the first one. The theoretical change of surface coverage distribution was calculated by integrating this equation. Then, the fitting procedures were performed with two parameters,  $D$  and  $\alpha$ .

Resultant fitted curves are shown as solid lines in Fig. 3(bottom), together with fitting results without the second process and coverage dependence (dashed lines). Obviously, the consideration of the second process is necessary to reproduce the observed distribution. As a result, the diffusion coefficient  $D$  was determined to be  $3.0 \pm 0.5 \mu\text{m}^2 \text{s}^{-1}$ , and the ratio  $\alpha$  was  $0.33 \pm 0.03$ . Thus, the diffusion coefficients of the first and second processes amount to  $(3.0 \pm 0.5) \times 10^{-12}$  and  $(9.9 \pm 2.5) \times 10^{-13} \text{m}^2 \text{s}^{-1}$ , respectively. Furthermore, the dwell time  $\tau$  of proton between two successive proton-transfer events was determined by using the relation  $D = \lambda^2/2\tau$ , where the term  $\lambda$  is the effective hopping length of each proton transfer [21]. The dwell time  $\tau$  for the simple proton transfer from H<sub>2</sub>O to adjacent OH was found to be  $5.2 \pm 0.9$  ns, and that for the H<sub>3</sub>O<sup>+</sup>-mediated one becomes  $48 \pm 12$  ns. Therefore, the proton transfer on a Pt(111) surface occurs with a time scale of nanosecond at 140 K. We also found that the rate of proton transfer via H<sub>3</sub>O<sup>+</sup> species is slower than that of the simple proton transfer by an order of magnitude. Note that these pathways of proton transfer are probably accompanied by proton-coupled electron transfer, leading to net effects of H migration. These processes are influenced by the Pt(111) surface as well as adsorbate configurations.

The diffusion coefficient of proton transfer in the three dimensional (3D) ice VII phase is ranged from  $10^{-17}$  to  $10^{-15} \text{m}^2 \text{s}^{-1}$  [7], which is much smaller compared to that on Pt(111) ( $10^{-13}$ – $10^{-12} \text{m}^2 \text{s}^{-1}$ ). The proton transfer in the solid acid CsHSO<sub>4</sub> also exhibits a smaller coefficient ( $10^{-14} \text{m}^2 \text{s}^{-1}$ ) [22]. On the other hand, the protonic diffusion in the liquid acid-base reaction proceeds much faster with the time scale from femto- to picosecond [3].



In the acid-base reactions in solution the degree of freedom available for proton transfer is relatively high, whereas it is limited in the solids; for example, in the  $\text{CsHSO}_4$  the reorientation of  $\text{SO}_4$  tetrahedra, which is necessary to forward the proton transfer, is a rate-limiting process, resulting in a slower time constant. The proton transfer in the present 2D-solid system shows an intermediate time scale between liquid and 3D-solid phases.

A recent time-resolved infrared spectroscopy study revealed proton itinerary into solvent water molecule(s) bridging the acid and base, which causes lowering of the transfer rate of protons [3,23]. In order to check such a solvent effect, we performed spatiotemporal tracing of an  $\text{OH} + \text{H}_2\text{O}/\text{H}_2\text{O}/\text{OH} + \text{H}_2\text{O}$  layer on Pt(111) after depositing multilayers of water at 140 K and consequently the diffusion coefficient was estimated to be  $0.29 \pm 0.07 \mu\text{m}^2 \text{s}^{-1}$  with the ratio  $\alpha$  of  $0.63 \pm 0.03$ . The rate of proton transfer is reduced by an order of magnitude in the presence of water multilayer. This might be explained by peripatetic behavior of proton into the  $\text{H}_2\text{O}$  molecule(s) which bridges two hopping sites on the surface.

In conclusion, the time scale of the proton transfer from  $\text{H}_2\text{O}$  to  $\text{OH}$  in the 2D hydrogen-bonding network on a Pt(111) surface was determined from micro-XPS observations of spatiotemporal changes in the patterned distribution  $\text{OH} + \text{H}_2\text{O}/\text{H}_2\text{O}/\text{OH} + \text{H}_2\text{O}$  initially prepared by the LITD method. The obtained spatiotemporal changes were explained based on the diffusion equation, taking account of two different pathways: the direct proton transfer to the neighbor site and the  $\text{H}_3\text{O}^+$ -mediated proton transfer to the next-nearest site. As a result, the time scales of the two proton-transfer pathways are found to be  $5.2 \pm 0.9$  ns and  $48 \pm 12$  ns, respectively, at 140 K. The rate of this 2D proton transfer is significantly lowered in the presence of water multilayers on top of the 2D system, which suggests proton itinerary into the water molecule(s) in the upper layer. The understanding of proton dynamics at the 2D interfaces will be important to the protonics at interfaces like fuel-cell electrodes and biological membranes.

This study was supported by the Grant-in-Aid for Scientific Research (No. 16072205 and No. 17205002). The present work has been performed under the approval of the Photon Factory Advisory Committee (PF PAC No. 2004G320 and No. 2006G355). One of the authors (M.N.) also acknowledges the support of the JSPS.

\*kondo@chem.s.u-tokyo.ac.jp

- [1] M.E. Tuckerman, D. Marx, and M. Parrinello, *Nature (London)* **417**, 925 (2002).
- [2] D.A. Boysen, T. Uda, C.R.I. Chisholm, and S.M. Haile, *Science* **303**, 68 (2004).
- [3] O.F. Mohammed, D. Pines, J. Dreyer, E. Pines, and E.T.J. Nibbering, *Science* **310**, 83 (2005).
- [4] H. Li, S.D. Mahanti, and T.J. Pinnavaia, *J. Phys. Chem. B* **109**, 21908 (2005).
- [5] S. Subramaniam and R. Henderson, *Nature (London)* **406**, 653 (2000).
- [6] T. Norby, *Nature (London)* **410**, 877 (2001).
- [7] E. Katoh, H. Yamawaki, H. Fujihisa, M. Sakashita, and K. Aoki, *Science* **295**, 1264 (2002).
- [8] M.A. Henderson, *Surf. Sci. Rep.* **46**, 1 (2002).
- [9] G.B. Fisher, J.L. Gland, and S.J. Schmieg, *J. Vac. Sci. Technol.* **20**, 518 (1982).
- [10] C. Sachs, M. Hildebrand, S. Völkening, J. Wintterlin, and G. Ertl, *Science* **293**, 1635 (2001).
- [11] C. Clay, S. Haq, and A. Hodgson, *Phys. Rev. Lett.* **92**, 046102 (2004).
- [12] A.P. Seitsonen, Y. Zhu, K. Bedürftig, and H. Over, *J. Am. Chem. Soc.* **123**, 7347 (2001).
- [13] G. Held, C. Clay, S.D. Barrett, S. Haq, and A. Hodgson, *J. Chem. Phys.* **123**, 064711 (2005).
- [14] A. Michaelides and P. Hu, *J. Am. Chem. Soc.* **123**, 4235 (2001).
- [15] M. Nagasaka, H. Kondoh, and T. Ohta, *J. Chem. Phys.* **122**, 204704 (2005).
- [16] K. Amemiya, H. Kondoh, T. Yokoyama, and T. Ohta, *J. Electron Spectrosc. Relat. Phenom.* **124**, 151 (2002).
- [17] H. Ogasawara, B. Brena, D. Nordlund, M. Nyberg, A. Pelmenschikov, L.G.M. Pettersson, and A. Nilsson, *Phys. Rev. Lett.* **89**, 276102 (2002).
- [18] The initial distribution was obtained 10 hours after preparing the modulated structure. After that, the most of excess water in the  $\text{H}_2\text{O}$  region might be desorbed.
- [19] S. Meng, *Surf. Sci.* **575**, 300 (2005).
- [20] M. Nagasaka, H. Kondoh, K. Amemiya, T. Ohta, and Y. Iwasawa (to be published).
- [21] The hopping length  $\lambda$  was estimated from the crystal surface rotation obtained by low energy electron diffraction and the distance  $l$  of the unit cell (2.8 Å). Those of the first and second processes were determined to be 1.77 and 3.07 Å, respectively.
- [22] M. Mizuno and S. Hayashi, *Solid State Ionics* **167**, 317 (2004).
- [23] O.F. Mohammed, D. Pines, E.T.J. Nibbering, and E. Pines, *Angew. Chem., Int. Ed.* **46**, 1458 (2007).